What Transmission Conditions are Algebraically Chosen by RAS?

Martin J. Gander[0000−0001−8450−9223], Laurence Halpern[0000−0002−7877−7130], and Lahcen Laayouni[0009−0000−5378−2825]

1 Introduction

In 1999, Cai and Sarkis introduced in a short note [1] the Restricted Additive Schwarz method (RAS), based on a small modification in an Additive Schwarz (AS) code: "we removed part of the communication routine and surprisingly the 'then AS' method converged faster both in terms of iteration counts and CPU time". This led to a wealth of research, and the success of RAS was so important that it is now the default Schwarz preconditioner in PETSc.

It was shown in [9] that RAS represents a faithful discretization of the parallel Schwarz method of Lions, and thus converges as a stationary iterative method, as Lions showed by maximum principle arguments in [14], even in the presence of cross points, where its variational interpretation does not hold[1]. In contrast, AS [3] is a preconditioner for Krylov methods, making a clever compromise between efficiency in the overlap and symmetry, and AS does not converge like the parallel Schwarz method of Lions without Krylov acceleration, see Figure 1, and [4] for a simple introduction. Note that the Multiplicative Schwarz method (MS) is equivalent to the discretization of the classical alternating Schwarz method [2], and Restricted Multiplicative Schwarz (RMS) and MS are equivalent [9].

Unfortunately, in contrast to AS, RAS is non-symmetric, and thus its convergence can not easily be analyzed in the context of the abstract Schwarz framework based on condition number estimates. There are algebraic convergence analyses based on

Martin J. Gander
Université de Genève, e-mail: martin.gander@unige.ch

Laurence Halpern
Université Sorbonne Paris Nord, e-mail: laurence.halpern@univ-paris13.fr

Lahcen Laayouni
Al Akhawayn University, e-mail: L.Laayouni@aui.ma

[1] "And even if, as we will see in section II, each sequence u_n^i converges in O_i to u, this method does not have always a variational interpretation in terms of iterated projections" [13, pages 18-19].

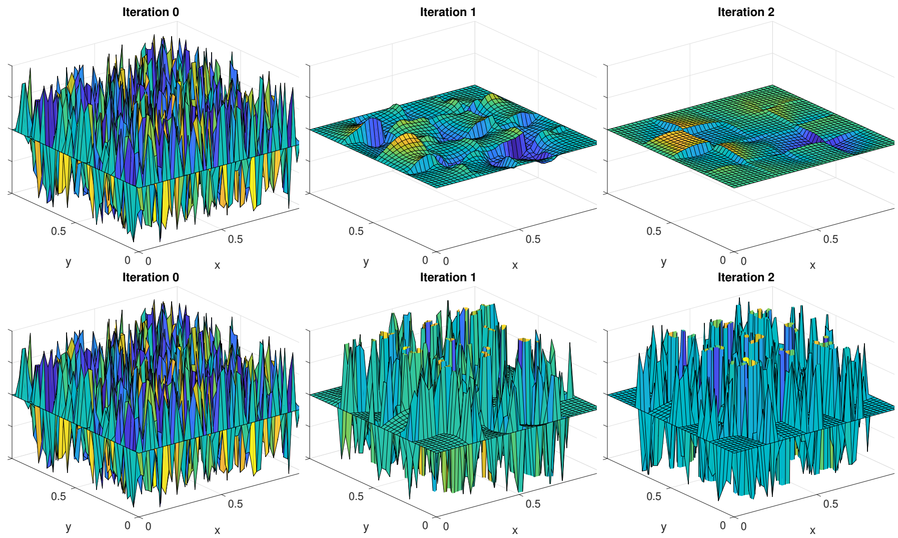

Fig. 1 Error for a 4 × 4 subdomain decomposition and the Laplace problem, four mesh sizes overlap, starting with random initial error. Top: Parallel Schwarz method of Lions ≡ RAS without Krylov acceleration. Bottom: Additive Schwarz without Krylov acceleration.

weighted maximum norms using M-matrix techniques in [5], albeit without leading to convergence rates. Very recently, a new technique was introduced in [16] to obtain convergence rate estimates using relaxation for RAS in 1D via its variant Additive Schwarz with Harmonic Extension (ASH). ASH has also been proved to be equivalent to the discretized parallel Schwarz method of Lions [11, 12] if there are no cross points in the decomposition, and then Lions' convergence analyses also apply to ASH.

Like AS, RAS is defined entirely at the algebraic level. If RAS is applied to a discretized PDE, and its restriction matrices are aligned with the mesh used for the discretization, then the equivalence results in [9] hold with the parallel Schwarz method of Lions. If the restriction operators are however not aligned with the mesh, e.g., they cut through high order element degrees of freedom, neither is it known what method RAS represents for the discretized PDE considered, nor how RAS converges. We study here precisely such a case, and show that RAS becomes a Schwarz method that does not use Dirichlet transmission conditions between subdomains.

Our work is related to a recent study on multigrid methods for DG discretizations of reaction diffusion equations [15], where cell block Jacobi smoothers and point block Jacobi smoothers are studied. Algebraically both are two by two block Jacobi methods in 1D, but the point one corresponds to taking the two (discontinuous) degrees of freedom between the DG elements for the two by two blocks, while the cell one corresponds to a Schwarz method with subdomains given by the DG elements, see also [7, 8] for an interpretation of optimized Schwarz methods then.

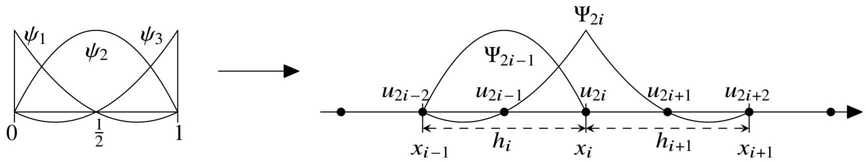

Fig. 2 $\mathbf{P}_2$ finite element local basis functions ψ_α (left) and global basis functions Ψ_i (right).

2 RAS for high order element discretizations

In order to understand what happens in RAS if one cuts a high order element, we apply such a finite element discretization to the one dimensional Poisson problem,

$$-\Delta u = f, \quad \text{in } \Omega := (0,1),\, u(0) = g^0 \text{ and } u(1) = g^1. \tag{1}$$

We divide the domain Ω into $N+1$ intervals representing the finite elements, with points x_i, $i = 0, \cdots, N+1$, and define $h_i := x_i - x_{i-1}$, see Figure 2 on the right. A $\mathbf{P}_p$ finite element method for solving (1) is based on a discrete variational formulation: define $u_h := g^0\Psi_0 + g^1\Psi_{(N+1)p} + w_h$, and find $w_h \in V_h^0$ such that $\forall v_h \in V_h^0$, $(w_h', v_h') + g^0(\Psi_0', v_h') + g^1(\Psi_{(N+1)p}', v_h') = (f, v_h)$. V_h is the finite element space, generated by the basis functions $(\Psi_0, \cdots, \Psi_{(N+1)p})$, and $V_h^0 = V_h \cap H_0^1(0,1)$ is generated by all Ψ_j except the first and the last. For $p = 1$ the basis functions are the well-known hat functions. The global basis functions Ψ_j are obtained by concatenation-translation-dilation from the local basis functions ψ_α. To understand the main point, it suffices to focus on the case $p = 2$, see Figure 2 for notations. Ψ_{2i} is supported in $[x_{i-1}, x_{i+1}]$, while Ψ_{2i-1} is supported in $[x_{i-1}, x_i]$. The functions ψ_α are defined using Lagrange interpolation polynomials, which in the case $p = 2$ are (see Figure 2 on the left)

$$\psi_1(x) = 2(\frac{1}{2} - x)(1 - x), \quad \psi_2(x) = 4x(1 - x), \quad \psi_3(x) = 2x(x - \frac{1}{2}).$$

We identify the function u_h with the vector of degrees of freedom $\mathbf{u} = (u_1, \cdots, u_{2N+1})$, where the even indices correspond to the mesh nodes and the odd indices to the mid-points. Setting $f_j := (f, \Psi_j)$, the discrete variational formulation becomes equivalent to a matrix equation when using as test functions the basis functions, namely

$$A\mathbf{u} = \mathbf{f} \Leftrightarrow \sum_{i=1}^{2N+1} (\Psi_i', \Psi_j')u_i = f_j - (\Psi_0', \Psi_j')g^0 - (\Psi_{2(N+1)}', \Psi_j')g^1,\ j = 1, \ldots, 2N+1. \tag{2}$$

Applying RAS with two subdomains to the linear system (2), one starts with an initial guess $\mathbf{u}^0$ and then computes for $n = 0, 1, \ldots$

$$\mathbf{u}^{n+1} = \mathbf{u}^n + \sum_{j=1}^{2} \tilde{R}_j^T A_j^{-1} R_j(\mathbf{f} - A\mathbf{u}^n), \tag{3}$$

where the rectangular restriction matrices R_j are parts of the identity I, and the $\tilde{R}_j$ are of the same size but with a partition of unity weighting the diagonal entries such that $\tilde{R}_1^T\tilde{R}_1 + \tilde{R}_2^T\tilde{R}_2 = I$, and the subdomain matrices are defined by $A_j := R_jAR_j^T$.

Let us first take a particular look at the formulation $\mathbf{P}_1$, and to be concrete, let $N := 10$, and $R_1 := I(1:5,:)$ and $R_2 := I(5:9,:)$. The line number $i = 5$ where RAS cuts the matrix is $-\frac{1}{h_5}u_4 + (\frac{1}{h_5}+\frac{1}{h_6})u_5 - \frac{1}{h_6}u_6 = f_5$. Denoting by $\mathbf{v}^n \approx \mathbf{u}(1:5)$ the RAS approximation on the first subdomain, and $\mathbf{w}^n \approx \mathbf{u}(5:9)$ the approximation on the second, RAS corresponds for the first subdomain to the iteration

$$-\frac{1}{h_5}v_4^n + (\frac{1}{h_5}+\frac{1}{h_6})v_5^n = f_5 + \frac{1}{h_6}w_6^{n-1}, \quad \textit{i.e. } v_6^n = w_6^{n-1}, \tag{4}$$

and similarly for the second. This shows that the first subdomain takes a Dirichlet boundary condition at x_6 from the second subdomain, imposed like the Dirichlet boundary condition g^1 on the right in the matrix formulation (2), and similarly for subdomain two. The corresponding subdomains at the continuous level are $\Omega_1 := (0, x_6)$ and $\Omega_2 := (x_4, 1)$, with overlap size $h_5 + h_6$, and RAS with one overlap at the algebraic level is thus a discretization of the parallel Schwarz method with Dirichlet transmission conditions imposed at x_4 and x_6 with two mesh sizes overlap. Since all lines in the matrix A are the same for $\mathbf{P}_1$ elements, RAS always corresponds to the discretization of the parallel Schwarz method in this case, see [4, 9] for more details.

This becomes more interesting with the finite elements $\mathbf{P}_2$, where the equations of even and odd index are different. The elementary matrix K of products of local basis functions, *i.e.* $K_{\alpha,\beta} = (\psi'_\alpha, \psi'_\beta)$, is given by

$$K = \begin{pmatrix} \frac{7}{3} & -\frac{8}{3} & \frac{1}{3} \\ -\frac{8}{3} & \frac{16}{3} & -\frac{8}{3} \\ \frac{1}{3} & -\frac{8}{3} & \frac{7}{3} \end{pmatrix}. \tag{5}$$

If we use the same matrix size as for the $\mathbf{P}_1$ example above, i.e. half the number of $\mathbf{P}_2$ elements (which means the mesh sizes h_j here are twice the size of the ones above in the $\mathbf{P}_1$ case), we obtain after assembly for the lines 3 to 7 in the linear system (2)

$$\begin{array}{lllllll}
\frac{K_{21}}{h_2}u_2 + \frac{K_{22}}{h_2}u_3 + & \frac{K_{23}}{h_2}u_4 & & & & & = f_3,\\
\frac{K_{31}}{h_2}u_2 + \frac{K_{32}}{h_2}u_3 + & (\frac{K_{33}}{h_2}+\frac{K_{11}}{h_3})u_4 + & \frac{K_{12}}{h_3}u_5 + & \frac{K_{13}}{h_3}u_6 & & & = f_4,\\
 & \frac{K_{21}}{h_3}u_4 + & \frac{K_{22}}{h_3}u_5 + & \frac{K_{23}}{h_3}u_6 & & & = f_5,\\
 & \frac{K_{31}}{h_3}u_4 + & \frac{K_{32}}{h_3}u_5 + & (\frac{K_{33}}{h_3}+\frac{K_{11}}{h_4})u_6 + & \frac{K_{12}}{h_4}u_7 + & \frac{K_{13}}{h_4}u_8 & = f_6,\\
 & & & \frac{K_{21}}{h_4}u_6 + & \frac{K_{22}}{h_4}u_7 + & \frac{K_{23}}{h_4}u_8 & = f_7.
\end{array}$$

If we split this system with RAS as in the $\mathbf{P}_1$ case at $i = 5$, the values w_6 and v_4 become again Dirichlet transmission conditions, $v_6^n = w_6^{n-1}$ and $w_4^n = v_4^{n-1}$, and RAS is equivalent to the discretization of the parallel Schwarz method of Lions as for $\mathbf{P}_1$; we say that *the splitting is aligned with the finite elements*. If we increase however the algebraic subdomains by one line, $R_1 := I(1:6,:)$ and $R_2 := I(4:9,:)$, then a completely new coupling arises from RAS; for example on the first subdomain, we get

$$\frac{K_{31}}{h_3}v_4 + \frac{K_{32}}{h_3}v_5 + (\frac{K_{33}}{h_3} + \frac{K_{11}}{h_4})v_6 + \frac{K_{12}}{h_4}w_7 + \frac{K_{13}}{h_4}w_8 = f_6. \quad (6)$$

At the n-th iteration of RAS, this corresponds on the right of the first subdomain to

$$\frac{K_{31}}{h_3}v_4^n + \frac{K_{32}}{h_3}v_5^n + (\frac{K_{33}}{h_3} + \frac{K_{11}}{h_4})v_6^n = f_6 - \frac{K_{12}}{h_4}w_7^{n-1} - \frac{K_{13}}{h_4}w_8^{n-1}. \quad (7)$$

It does not make sense to interpret this as two Dirichlet conditions imposed on the first subdomain, $v_7^n = w_7^{n-1}$ and $v_8^n = w_8^{n-1}$ as in the $\mathbf{P}_1$ case, since one can not impose two Dirichlet boundary conditions on the Poisson subdomain problem. In order to understand what transmission conditions this corresponds to, we use the fact that on the other subdomain in RAS, the same equation (6) at iteration $n-1$ is satisfied in the interior of the subdomain, but with all w variables, i.e.

$$\frac{K_{31}}{h_3}w_4^{n-1} + \frac{K_{32}}{h_3}w_5^{n-1} + (\frac{K_{33}}{h_3} + \frac{K_{11}}{h_4})w_6^{n-1} + \frac{K_{12}}{h_4}w_7^{n-1} + \frac{K_{13}}{h_4}w_8^{n-1} = f_6,$$

and we can thus isolate using this equation the variables which are transmitted to subdomain Ω_1, i.e.

$$f_6 - \frac{K_{12}}{h_4}w_7^{n-1} - \frac{K_{13}}{h_4}w_8^{n-1} = \frac{K_{31}}{h_3}w_4^{n-1} + \frac{K_{32}}{h_3}w_5^{n-1} + (\frac{K_{33}}{h_3} + \frac{K_{11}}{h_4})w_6^{n-1} =: B_v(\mathbf{w}^{n-1}),$$

where we introduced the new transmission operator B_v. We can thus introduce this result into the equation (7) for $\mathbf{w}^n$, and using again the transmission operator B_v, we get as transmission conditions chosen by RAS

$$B_v(\mathbf{v}^n) = B_v(\mathbf{w}^{n-1}) \quad \text{and similarly} \quad B_w(\mathbf{w}^n) = B_w(\mathbf{v}^{n-1}), \quad (8)$$

with the corresponding operator $B_w(\mathbf{w}^n) := (\frac{K_{33}}{h_2} + \frac{K_{11}}{h_3})w_4^n + \frac{K_{12}}{h_3}w_5^n + \frac{K_{13}}{h_3}w_6^n$ for the other subdomain. We therefore found that cutting with the Schwarz method a higher order finite element at the algebraic level implies coupling conditions like (8) which look rather different from the Dirichlet coupling conditions $v_6^n = w_6^{n-1}$ and $w_4^n = v_4^{n-1}$. It is therefore of interest to study how the transmission conditions B_v and B_w affect the convergence of such Schwarz methods, and if one can do better by changing the transmission operators from the ones decided by the algebraic cutting of the matrix with RAS.

To see to what kind of transmission condition (8) corresponds to, we must interpret (7) as a boundary condition that is imposed. We therefore perform in the interval $[x_2, x_3]$ a Taylor expansion of order 2 at the point $x = x_3$ (in our example) of the function v whose components on the basis functions are v_4, v_5, v_6,

$$v_4 \sim v(x - h_3) = u(x) - h_3 v'(x) + \frac{h_3^2}{2}v''(x) + o(h_3^2),$$
$$v_5 \sim v(x - \frac{h_3}{2}) = v(x) - \frac{h_3}{2}v'(x) + \frac{h_3^2}{8}v''(x) + o(h_3^2).$$

Inserting this into $B_v(\mathbf{v})$, and replacing the coefficients $K_{\alpha,\beta}$, we obtain

$$B_v(\mathbf{v}) \sim \frac{7}{3h_4}v(x_3) + v'(x_3) - \frac{h_3}{6}v''(x_3), \tag{9}$$

which is a Robin transmission condition up to order h with Robin parameter $\frac{7}{3h_4}$. Similarly,

$$B_w(\mathbf{w}) \sim \frac{7}{3h_2}w(x_2) - w'(x_2) - \frac{h_3}{6}w''(x_2). \tag{10}$$

We have therefore proved the following result:

Proposition 1 *Algebraic RAS with $\mathbf{P}_2$ finite elements for $R_1 = I(1:2J+1,:)$ and $R_2 = I(2J+1:2N+1,:)$ gives the classical Schwarz method for $\Omega_1 = (0, x_{J+1})$ and $\Omega_2 = (x_J, 1)$. If however the restriction matrices are defined by $R_1 = I(1:2J+2,:)$ and $R_2 = I(2J:2N+1,:)$, then RAS is an approximation of a new Schwarz method on the same (!) subdomains $\Omega_1 = (0, x_{J+1})$ and $\Omega_2 = (x_J, 1)$ defined by*

$$\begin{array}{llll} -\Delta u_1^n = f & \text{in } \Omega_1, & -\Delta u_2^n = f & \text{in } \Omega_2, \\ \mathcal{B}_v u_1^n = \mathcal{B}_v u_2^{n-1} & \text{at } x = x_{J+1}, & \mathcal{B}_w u_2^n = \mathcal{B}_w u_1^{n-1} & \text{at } x = x_J, \end{array} \tag{11}$$

where the transmission operators chosen by RAS are (∂_n is the outward normal derivative)

$$\mathcal{B}_v(u) = \partial_n u + \frac{7}{3h_{J+1}}u - \frac{h_J}{6}\partial_{nn}u + \ldots, \quad \mathcal{B}_w(u) = \partial_n u + \frac{7}{3h_{J-1}}u - \frac{h_J}{6}\partial_{nn}u + \ldots, \tag{12}$$

i.e. a method of optimized Schwarz type with Robin transmission conditions, slightly perturbed with the higher order term.

For higher order $\mathbf{P}_p$ finite elements, there are many more possibilities to cut the matrix using RAS, as indicated graphically in Figure 3 on the left, where we represent the assembled system matrix by the brown boxes labeled with the local stiffness matrices K. There is always a choice corresponding to a classical Schwarz method, e.g. with one element overlap indicated in green in Figure 3 on the left: the first subdomain Ω_1 contains three higher order elements, i.e. three assembled matrices K. The last matrix K has its last row and column cut off by the green subdomain boundary, which means it takes Dirichlet values along this last column from the neighboring subdomain Ω_2, as in the $\mathbf{P}_2$ example above. Similarly for the second subdomain Ω_2 indicated by the other two green lines, it contains three higher order element matrices K, and the first one has its first row and column cut off. It thus takes there Dirichlet data from the neighboring subdomain, and we would say that *the RAS splitting is aligned with the higher order finite elements*.

If we cut however algebraic subdomains not aligned with the higher order elements, like for example the red lines in Figure 3 on the left which represent an algebraic subdomain choice $\tilde{\Omega}_1$ which is overlapping just one unknown more with the subdomain Ω_2, or the magenta subdomain $\tilde{\tilde{\Omega}}_1$ that cuts right in the middle of the higher order element stiffness matrix K, RAS will generate different transmission conditions from the classical Dirichlet ones, as in our $\mathbf{P}_2$ example in Proposition 1, and there are too many to be analyzed in detail in this short note.

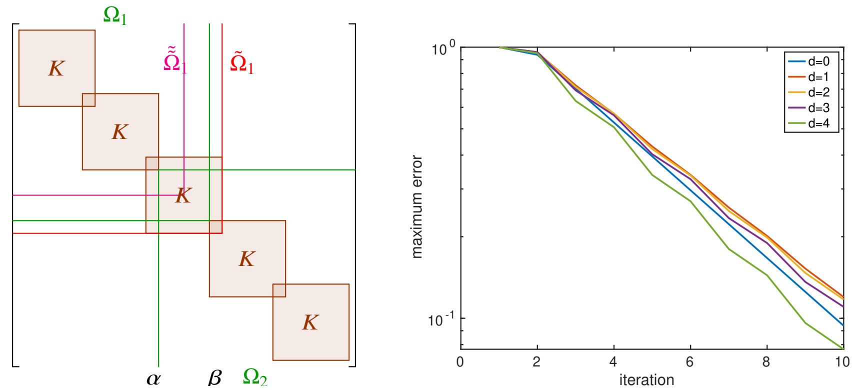

Fig. 3 Left: different possible subdomains depending on the restriction operators chosen in RAS. Right: Numerical experiment for seven $\mathbf{P}_5$ elements, cutting in the middle with one element overlap ($d = 0$) and then shifting both interfaces to the right ($d = 1, 2, 3, 4$).

Furthermore, in Proposition 1, we have shown that these transmission conditions are of Robin type, but the parameters are chosen by the RAS splitting. In optimized Schwarz methods, one chooses transmission conditions of the same form, but in order to obtain fast convergence, and from the analysis in [6], the Robin parameter chosen quite arbitrarily by RAS above is not very good for the performance of the Schwarz method: replacing $\frac{7}{6h}$ by $h^{-\frac{1}{3}}$ would lead to much faster convergence in 2D. The next term in the expansion, $-\frac{h}{3}u_{nn}(x)$, could be interpreted in the 2D Poisson case as a Ventcell term, since then $\partial_{nn} = -\partial_{\tau\tau}u - f$ using the properties of the Laplace operator, where $\partial\tau$ denotes the tangential derivative. However again, the value for the parameter chosen by RAS is not very good, it even has the wrong sign, there are much better choices, see [6].

3 Numerical experiments

We show in Figure 3 on the right a numerical experiment performed for a $\mathbf{P}_5$ element discretization of the 1D Poisson problem (1) using seven such finite elements. In this case, we can obtain several RAS variants by starting with aligned restriction matrices R_j with the $\mathbf{P}_5$ elements denoted by $d = 0$, as indicated in green in Figure 3 on the left, and then shifting the indices in both restriction matrices R_1 and R_2 to the right, i.e. increasing the size of R_1 and decreasing the size of R_2, denoted by $d = 1, 2, 3, 4$. The error plotted as a function of iteration index n in Figure 3 on the right shows that indeed these methods converge differently: the fastest two are the ones aligned with true geometric subdomains (green and blue). In all cases however much faster methods could be obtained changing the corresponding entries in the subdomain matrices A_j. While this has been analyzed in detail for $\mathbf{P}_1$ finite elements and led to Optimized RAS (ORAS) [17] and new, interesting preconditioning results [10], it remains largely unexplored for higher order $\mathbf{P}_p$ element discretizations.

References

1. Cai, X.C., Sarkis, M.: A restricted additive Schwarz preconditioner for general sparse linear systems. SIAM Journal on Scientific Computing **21**(2), 792–797 (1999)
2. Chan, T.F., Mathew, T.P.: Domain decomposition algorithms. Acta Numerica **3**, 61–143 (1994)
3. Dryja, M., Widlund, O.: An additive variant of the Schwarz alternating method for the case of many subregions. Ultracomputer Research Laboratory, Courant Institute of Mathematical Sciences (1987)
4. Efstathiou, E., Gander, M.J.: Why restricted additive Schwarz converges faster than additive Schwarz. BIT Numerical Mathematics **43**(5), 945–959 (2003)
5. Frommer, A., Szyld, D.B.: An algebraic convergence theory for restricted additive Schwarz methods using weighted max norms. SIAM Journal on Numerical Analysis **39**(2), 463–479 (2001)
6. Gander, M.J.: Optimized Schwarz methods. SIAM Journal on Numerical Analysis **44**(2), 699–731 (2006)
7. Gander, M.J., Hajian, S.: Analysis of Schwarz methods for a hybridizable discontinuous Galerkin discretization. SIAM Journal on Numerical Analysis **53**(1), 573–597 (2015)
8. Gander, M.J., Hajian, S.: Analysis of Schwarz methods for a hybridizable discontinuous Galerkin discretization: the many-subdomain case. Mathematics of Computation **87**(312), 1635–1657 (2018)
9. Gander, M.J., et al.: Schwarz methods over the course of time. Electron. Trans. Numer. Anal **31**(5), 228–255 (2008)
10. Haferssas, R., Jolivet, P., Nataf, F.: An additive Schwarz method type theory for Lions's algorithm and a symmetrized optimized restricted additive Schwarz method. SIAM Journal on Scientific Computing **39**(4), A1345–A1365 (2017)
11. Kwok, F.: Is Additive Schwarz with Harmonic extension just Lions' method in disguise? In: Domain Decomposition Methods in Science and Engineering XIX, pp. 439–446. Springer (2011)
12. Kwok, F.: Optimized additive Schwarz with harmonic extension as a discretization of the continuous parallel Schwarz method. SIAM Journal on Numerical Analysis **49**(3), 1289–1316 (2011)
13. Lions, P.L.: On the Schwarz alternating method. I. In: First international symposium on domain decomposition methods for partial differential equations, vol. 1, p. 42. Paris, France (1988)
14. Lions, P.L.: On the Schwarz alternating method. II. In: T. Chan, R. Glowinski, J. Périaux, O. Widlund (eds.) Domain Decomposition Methods, pp. 47–70. SIAM, Philadelphia, PA (1989)
15. Lorca, J.P.L., Gander, M.J.: Optimization of two-level methods for DG discretizations of reaction-diffusion equations. ESAIM: Mathematical Modelling and Numerical Analysis (2024)
16. Sarkis, M., Dryja, M.: Convergence bounds for one-dimensional ASH and RAS. In: Domain Decomposition Methods in Science and Engineering XVII, pp. 39–50. Springer (2022)
17. St-Cyr, A., Gander, M.J., Thomas, S.J.: Optimized multiplicative, additive, and restricted additive Schwarz preconditioning. SIAM Journal on Scientific Computing **29**(6), 2402–2425 (2007)